Walking the tightrope of bioavailability: growth dynamics of PAH degraders on vapour-phase PAH

Joanna Hanzel, Martin Thullner, Hauke Harms and Lukas Y. Wick*

UFZ – Helmholtz Centre for Environmental Research, Department of Environmental Microbiology, 04318 Leipzig, Germany.

Summary

Microbial contaminant degradation may either result in the utilization of the compound for growth or act as a protective mechanism against its toxicity. Bioavail-ability of contaminants for nutrition and toxicity has opposite consequences which may have resulted in quite different bacterial adaptation mechanisms; these may particularly interfere when a growth sub-strate causes toxicity at high bioavailability. Recently, it has been demonstrated that a high bioavailability of vapour-phase naphthalene (NAPH) leads to chemo-tactic movement of NAPH-degrading *Pseudomonas putida* (NAH7) G7 away from the NAPH source. To investigate the balance of toxic defence and substrate utilization, we tested the influence of the cell density on surface-associated growth of strain PpG7 at differ-ent positions in vapour-phase NAPH gradients. Con-trolled microcosm experiments revealed that high cell densities increased growth rates close (< 2 cm) to the NAPH source, whereas competition for NAPH decreased the growth rates at larger distances despite the high gas phase diffusivity of NAPH. At larger distance, less microbial biomass was likewise sustained by the vapour-phase NAPH. Such varying growth kinetics is explained by a combination of bio-availability restrictions and NAPH-based inhibition. To account for this balance, a novel, integrated 'Best Equation' describing microbial growth influenced by substrate availability and inhibition is presented.

Introduction

Effective biodegradation of soil contaminants requires both adequate environmental conditions and a suitable availability of the compounds to the degrading organisms.

The average bulk concentration of a contaminant, however, is not an appropriate measure for its availability, since bioavailability needs to be seen as the dynamic interplay of the mass transfer (flux) of a compound to a microbial cell and its metabolic potential to degrade it (Bosma *et al.*, 1997). At high transfer rates, degradation hence is predominantly controlled by the metabolic poten-tial of the bacteria, whereas low transfer rates may limit both the microbial growth rates and the amount of biomass sustained. Reversibly, the bioavailability may also become limiting when the catabolic capacity of a microbial biomass exceeds the capacity of its environ-ment to deliver it, as often can be found in soil environ-ments (Johnsen *et al.*, 2005). The bioavailability of a compound can adequately be quantified by the bioavail-ability number (*Bn*) which takes into account the mass transfer of a compound to microbial cells and the intrinsic activity of these cells to transform it (Bosma *et al.*, 1997). For the assumed situation of steady state (i.e. when the transport flux and the rate of degradation of the substrate equal each other) the so-called Best Equation (Best, 1955) describes substrate uptake in relation to the con-taminant mass transfer potential in the environment sur-rounding a cell, i.e. it evaluates the relative physical and biological contributions to the overall degradation rate.

Microbial contaminant degradation may either result in the utilization of the contaminant for growth or contribute to the protection against contaminant toxicity depending on its flux to individual cells. The bioavailability of a com-pound hence is 'Janus-faced', i.e. bioavailability is essen-tial and likely promoted by the target organism for assimilative uptake, whereas a too high bioavailability of a compound may lead to toxic effects and provoke avoid-ance strategies of the target organisms. Although the bioaccessible compound pool for both effects may be identical, the exposure of organisms to environmental chemicals hence has opposite consequences and may lead to quite different bacterial adaptation mechanisms depending on the compounds bioavailability. These may interfere, when a growth substrate causes toxicity at high bioavailability, leading to a tightrope walk that is often overlooked in bioremediation studies where one tends to assume that effective pollutant-utilizing bacteria tolerate any exposure to these substrates. Intracellular NAPH, for instance, has been reported to be toxic to *Pseudomonas putida* (NAH7) G7 unless it is metabolized (Ahn *et al.*,

1998), e.g. under oxygen-, nitrogen- or nutrient-limiting conditions (Ahn *et al.*, 1998; Park *et al.*, 2004; Pumphrey and Madsen, 2007). According to Pumphrey and Madsen (2007) likely hypotheses for explaining the inhibitory effect of NAPH are: (i) NAPH itself is directly inhibitory or toxic when present at high concentrations, (ii) the NAPH metabolism leads to the accumulation of toxic or inhibitory metabolites [or reactive oxygen species (George and Hay, 2011)] at elevated NAPH bioavailability to the cells, or (iii) both NAPH and its metabolites cause growth inhibition. Recently, it also has been demonstrated in controlled laboratory systems that the high bioavailability of vapour-phase NAPH induced negative chemotaxis, i.e. a down-gradient movement of NAPH-degrading *P. putida* (NAH7) G7 away from a solid NAPH point source. Surprisingly, this occurred even at gaseous concentrations lower than aqueous concentrations that induced chemoattraction (Hanzel *et al.*, 2010).

Knowledge of how and where microbial populations develop in vapour phase-substrate gradients is of great importance for a better understanding of the degradation of volatile organic compounds (VOC), as found for instance in the vadose zone of terrestrial environments. The goal of this study was (i) to experimentally elucidate the tightrope walk of substrate bioavailability for assimilative growth and growth inhibition of strain PpG7 in vapour-phase NAPH gradients and (ii) to qualitatively reflect microbial growth in a novel kinetic model combining assimilative growth driven by substrate (bio-)availability and inhibition/toxicity.

Results

Growth on vapour-phase NAPH

Growth of NAPH-degrading strain *P. putida* (NAH7) G7 on the surface of agar exposed to vapour-phase NAPH was studied in Petri dish microcosms with an emphasis on influences of cell density and distribution. As illustrated in Figs. 1A and S1A, all microcosms contained a central minimal medium agar (MMA) disk (A) and/or concentric MMA rings of varying diameters (B, C, D), which were positioned at various distances from the central NAPH point source. Two different inoculation patterns were tested allowing for distinct NAPH fluxes to individual bacteria due to a varying overall consumption of and competition for vapour-phase NAPH at the cm scale: in a '*high-competition*' scenario (HCS) (Figs. 1B and S1B) all agar patches (A–D) were simultaneously present and homoge-
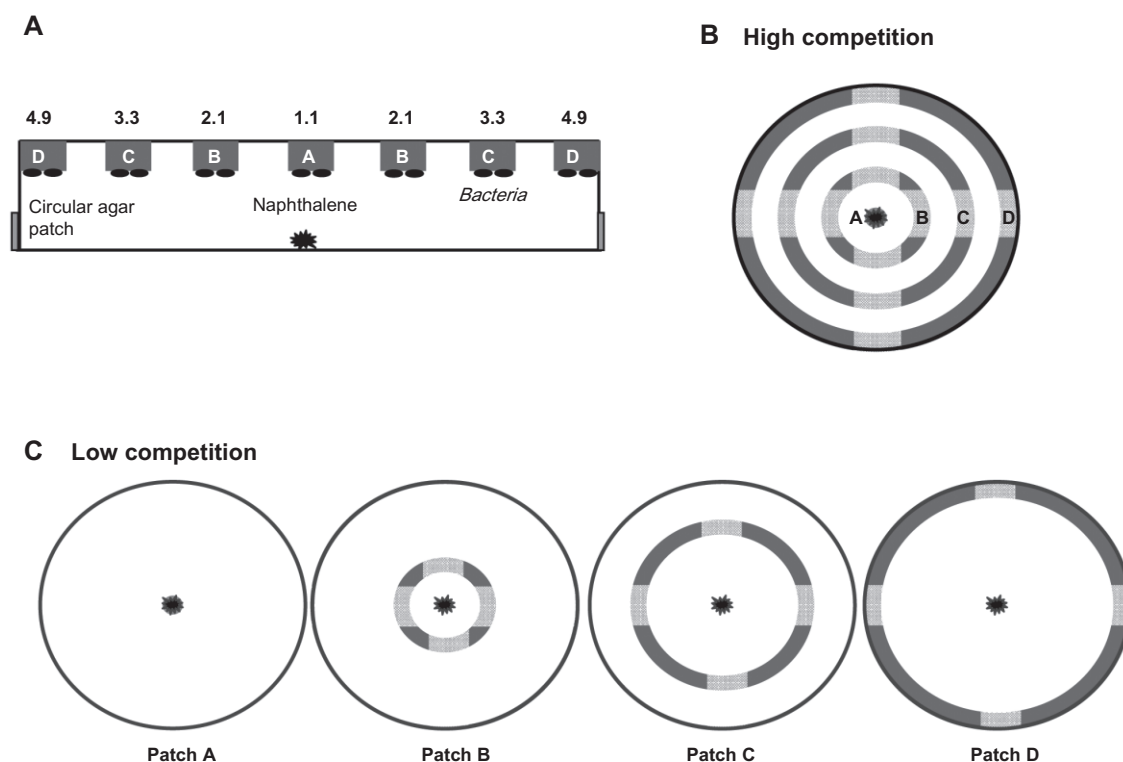
Fig. 1. Cross-section (A) and birds view (B) of the experimental set-up for studying growth of NAPH-degrading surface-associated *Pseudomonas putida* (NAH7) G7 on vapour-phase NAPH of variable bioavailability. The numbers in (A) refer to the average distances in cm of the patches sampled to the solid NAPH. (B) shows the experimental scenario to assess for increased inter-microbial competition ('high competition', sampling locations are symbolized by the light-coloured areas), whereas (C) depicts the four scenarios to mimic lower competition scenarios ('low competition, sampling locations are symbolized by the light-coloured areas).
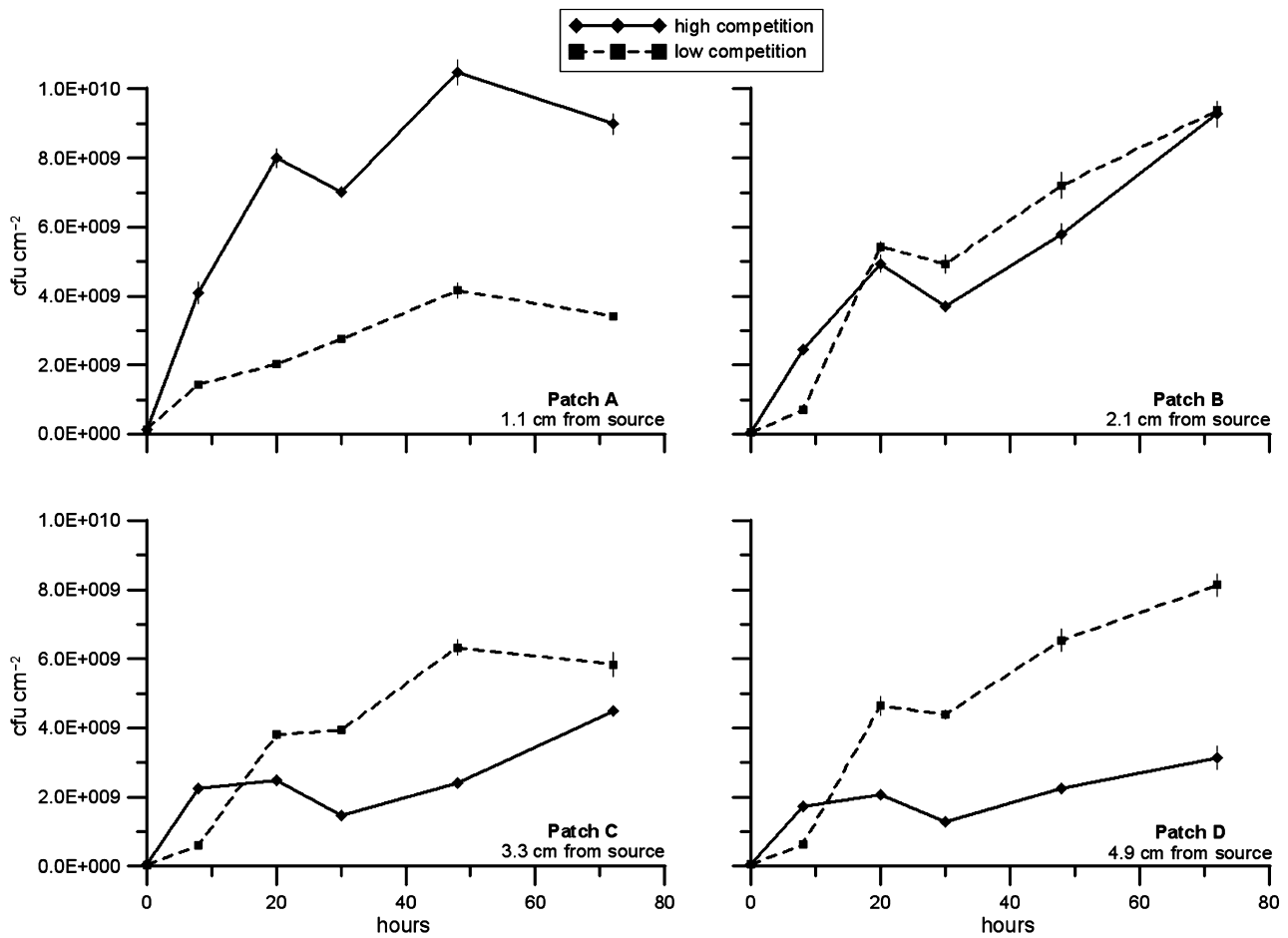
Fig. 2. Spatiotemporal growth of MMA surface-associated *P. putida* (NAH7) G7 on vapour-phase NAPH at different distances (patch A, B, C and D, i.e. at 1.1, 2.1, 3.3 and 4.9 cm) from the NAPH spot source at conditions mimicking high (diamonds) and low (squares) microbial competition. Growth is reflected by cfu that are surface area normalized and represent averages and standard errors (1 sigma) from four locations taken of MMA patches obtained from three independent experiments.

neously inoculated with 4.5×10^8 colony-forming unit (cfu) cm^{-2}, whereas in 'low-competition' scenarios (LCS) each of the equally inoculated patches (A, B, C or D) was placed in a separate Petri dish (Figs. 1C and S2). Similar to previous studies vapour-phase NAPH emanating from the point source led to cm-scale vapour-phase NAPH gradients (cf. Hanzel *et al*., 2010; 2011) as expressed by distinct biomass distribution patterns after 8, 20, 30, 48 and 72 h of incubation (Fig. 2). The biomass was approximated by cfu analysis on LB agar after sacrificing the individual patches. The cfu data reveal that higher total numbers of widely distributed cells in the HCS facilitated growth close to the NAPH source (A and B) with three times higher cell numbers per cm^2 than at more distant locations (C and D). In the LCS, growth on patch A was at least 60% lower than in the HCS at all sampling times. Lower biomass than in the HCS was detected after 8 h on all patches (A–D) in the LCS (Fig. 2). With increasing cell numbers and NAPH consumption in the LCS, the biomass

in position B became similar in both scenarios and even exceeded that in the HCS by up to 60% on patches C and D.

An analysis of average growth rates until 72 h further illustrates these effects (Fig. 3). The different inoculum pattern in the HCS led to an about twofold accelerated growth rate of the cells on patch A, yet kept the growth rate of the cells on patch B uninfluenced, or reduced it by about 60% at more distant locations from the NAPH source (patches C and D; Fig. 3).

Kinetic description of bacterial growth influenced by substrate toxicity and competition

To explain the observed growth patterns in terms of microbial growth kinetics, we modified an established concept for growth under bioavailability restrictions so that it accounts for toxic growth inhibition. When transport flux and the rate of substrate degradation equal
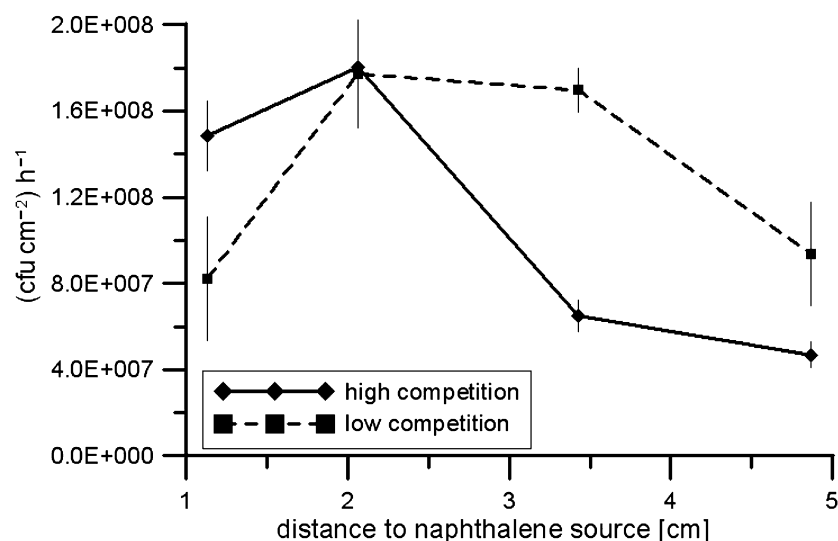
Fig. 3. Spatially resolved growth rates of *P. putida* (NAH7) G7 during 72 h of growth on vapour-phase NAPH emanating from a spot source. High- and low-competition experiments are represented by diamonds and squares respectively. Data represent averages and standard errors from three independent experiments.

each other (i.e. at quasi-steady-state conditions) the so-called Best Equation (Best, 1955) describes the relative physical and biological contributions to the overall degradation rate. In the following, an extended version of this concept is proposed which allows for the description of microbial growth in a domain where substrate consumption for assimilation and for detoxification occurs. The dynamics of bacterial substrate degradation is commonly expressed using Michaelis–Menten kinetics (Lehninger *et al.*, 2004):

$$r_{deg} = k_m \cdot \frac{c_b}{K_s + c_b} \quad (1)$$

with k_m as maximum degradation rate per unit biomass, K_s as Michaelis–Menten constant and c_b as the bioavailable concentration of the substrate. If the bioavailable concentration differs from the total bulk concentration c_{tot} of the substrate, i.e. if bioavailability restrictions need to be considered, the link between these two concentrations can be expressed using a linear exchange model (Baveye and Valocchi, 1989; Button, 1991; Thullner *et al.*, 2007; Hesse *et al.*, 2010) describing the exchange rate r_{ex}:

$$r_{ex} = \lambda \cdot (c_{tot} - c_b) \quad (2)$$

with λ as exchange rate parameter influenced by the mass transfer processes controlling substrate bioavailability. Typically, λ increases with the mobility (e.g. diffusion coefficient) of the substrate and decreases with the distance to be covered by the mass transfer process. When rates for mass flux and substrate degradation equal each other and assuming (quasi-)steady-state conditions at the micro scale ($r_{deg} = r_{ex}$), Eqs 1 and 2 can be combined to the so-called

Best Equation (Best, 1955; Bosma *et al.*, 1997; Simoni *et al.*, 2001),

$$r_{Best} = \frac{K_s \lambda}{2} \cdot \left(1 + \frac{c_{tot}}{K_s} + \frac{k_m}{K_s \lambda}\right) \cdot \left[1 - \sqrt{1 - \frac{4\frac{c_{tot}}{K_s}\frac{k_m}{K_s \lambda}}{\left(1 + \frac{c_{tot}}{K_s} + \frac{k_k}{K_s \lambda}\right)^2}}\right] \quad (3)$$

which allows expressing the degradation rate as a function of the bulk concentration in the presence of bioavailability restrictions. The smaller the bulk concentration and the smaller the bioavailability number $Bn = K_s \lambda / k_m$ the higher the influence of bioavailability restriction on the degradation rate. The above concept is valid and established if the substrate is the only rate limiting substance and if high substrate concentrations have no inhibitory effects on the degradation rate. To address the latter – as necessary for the present study – the simple Michaelis–Menten kinetics (Eq. 1) needs to be expanded. From the different approaches proposed to include such inhibition terms into growth rate expressions we here discuss an example:

$$r_{deg} = k_m \cdot \frac{c_b}{K_s + c_b} \cdot \frac{K_i}{c_b + K_i} \quad (4)$$

proposed for non-competitive inhibition (Lehninger *et al.*, 2004), with K_i as inhibition constant. Equation 4 is also commonly used to address inhibition effects in reactive transport simulations (Thullner *et al.*, 2007). To combine this expanded rate expression with bioavailability restrictions (Eq. 2) in analogy to the above derivation of the Best Equation leads to bioavailable concentrations fulfilling the equation
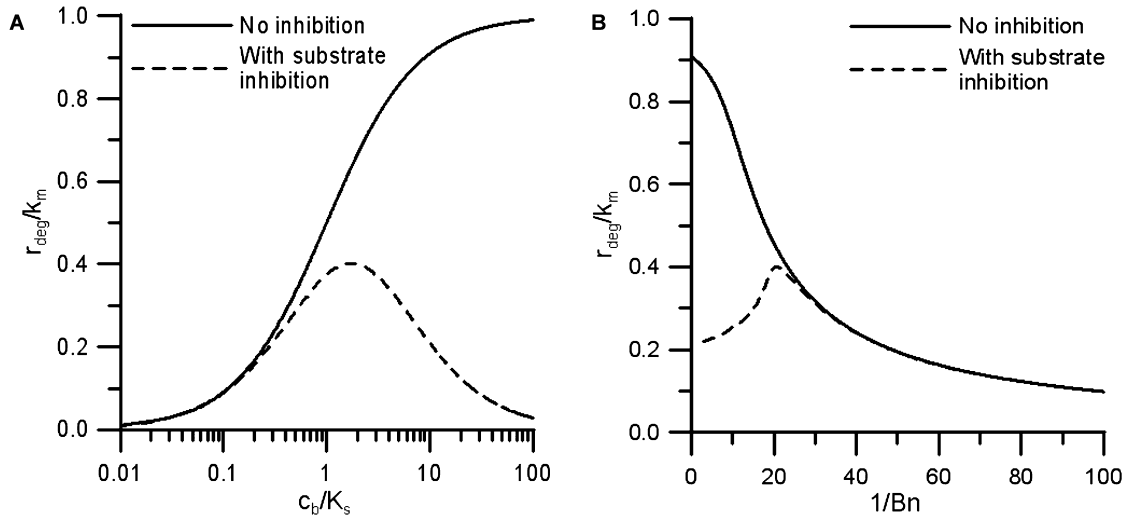
Fig. 4. Influence of substrate inhibition on microbial degradation (and growth) rates.
A. Rate dependence on bioavailable substrate concentration considering the presence (Eq. 4) and absence of substrate inhibition effects (Eq. 1) assuming $K_i = 3K_s$.
B. Rate dependence on bioavailable substrate concentration as expressed by the bioavailability number *Bn* considering the presence (Eq. 5 combined with Eq. 2 or 4) and absence (Eq. 3) of substrate inhibition effects assuming $c_{tot} = 10K_s$ and $K_i = 3K_s$. Note that high bioavailability is represented by low values of 1/*Bn*.

$$c_b{}^3 + (1 + c_{tot} + K_i) \cdot c_b{}^2 +$$
$$\left[K_s \cdot K_i + \frac{K_i \cdot k_m}{\lambda} - (K_i + K_s) \cdot c_{tot} \right] \cdot c_b - K_s \cdot K_i \cdot c_{tot} = 0 \quad (5)$$

It is not possible to express the general solution of Eq. 5 and the resulting degradation rate in a closed form (which would be an expanded Best Equation considering inhibition effects, too). However, for specific parameter values a numerical solution for c_b can be obtained from Eq. 5, which can then be used to calculate rate values using Eq. 2 or 4. The link between the growth rate of a bacterial species B and the above presented degradation rates is the given assuming a constant yield factor *Y*:

$$\frac{\partial B}{\partial t} = Y \cdot r_{deg} \cdot B \quad (6)$$

which in the simplest case (Michaelis–Menten kinetics, no bioavailability restriction, no inhibition effects) results in the established Monod-type growth kinetics (Monod, 1949; Thullner *et al.*, 2007), or in an extended version of it considering bioavailability and substrate inhibition.

The theoretically predicted influence of substrate inhibition on degradation rates is shown for an arbitrary but representative example (Fig. 4A) to demonstrate the differences between the considered rate expressions (Eq. 1 in the absence of inhibition effects, and Eq. 4 in the presence of inhibition effects). Omission of inhibition effects results in a rate monotonously increasing with substrate concentration. In turn, when consideration of inhibition effects leads to predicted maximum rates at a concentration of $c_b = (K_i \cdot K_s)^{1/2}$. At concentrations of $c_b < (K_i \cdot K_s)^{1/2}$ the rate is decreasing due to substrate limitation while higher concentrations of $c_b > (K_i \cdot K_s)^{1/2}$ lead to a rate decrease due to substrate inhibition. Similar observations were made using alternative expressions suggested in the literature (e.g. Mulchandani and Luong, 1989) to describe rate inhibition effects (results not shown). Figure 4B relates the influence of inhibition to changes of the substrate degradation rates (and hence of bacterial growth rates) at varying substrate bioavailability conditions. In the absence of inhibition degradation rates are highest when the substrate is highly bioavailable (i.e. lower values for 1/*Bn*), whereas reduction of substrate bioavailability (e.g. due to increased distance or increased competition as in the LCS or HCS) leads to concomitant decrease of the degradation rates. Interestingly, the degradation rates at all bioavailability conditions (values of 1/*Bn*) are lower in the presence of inhibition (Fig. 4A and B). While at low bioavailability inhibition effects remain small, differences grow significantly larger at high bioavailability conditions. Figure 4B further reveals that inhibition leads to highest degradation rates at intermediate substrate bioavailability conditions representing a compromise of moderate inhibition and sufficient substrate supply to a metabolically active cell.

Discussion

Bacterial growth influenced by substrate toxicity and competition

In an attempt to evaluate the microbial utilization of a potentially inhibitory vapour-phase substrate, we tested influences of initial biomass and its location relative to an NAPH point source. Our data reveal that growth rates of *P. putida* depended on their distance to the NAPH source and were influenced by the spatial distribution and abundance of catabolically active cells in the microcosm. This is explained by the formation of cm-scale, vapour-phase NAPH gradients forming around an NAPH point source, which (despite of the high diffusivity of NAPH in air) have previously been demonstrated in similar laboratory test tracks likewise using strain PpG7 (Hanzel *et al.*, 2010; 2011). In these studies the volatilization of NAPH from a solid spot source resulted in distinct gradients in the headspace of a Petri dish with average vapour-phase NAPH concentrations near the source close to the equilibrium concentration ($\approx 3 \times 10^{-7}$ mol l^{-1}) and an approximately threefold drop along a Petri dish's transect (Hanzel *et al.*, 2010). Petri dishes hence emerge as ideal experimental reactors to study the spatiotemporal interplay of varying NAPH bioavailability and microbial growth. Our data are in good agreement with previous studies considering bioavailability as a dynamic process influenced by the rate of physical mass transfer to microbial cells relative to their intrinsic catabolic activity (e.g. Bosma *et al.*, 1997; Wick *et al.*, 2001). As convection is apparently absent in our closed microcosms, the NAPH flux is best described by Fick's first law of diffusion (Schwarzenbach *et al.*, 2003) implying that bioavailability of vapour-phase NAPH decreases with distance as has been demonstrated in a recent study (Hanzel *et al.*, 2011). The higher amount of bacterial cells present in the HCS leads to a reduced per cell bioavailability of NAPH compared with the LCS [as previously has been demonstrated for the degradation of dissolved toluene by suspended bacteria (Kampara *et al.*, 2009)]. The complex effect of additional biomass results from the fact that additional NAPH consumption reduces toxicity under conditions of high bioavailability. It thus either buffers toxic effects by removing vapour-phase NAPH or intensifies the competition for substrate. Figures 2 and 3 indicate that bacteria located close to the NAPH source benefit from the buffer effect of additional biomass, while those located at larger distances suffer from additional competitors. The position of the transition zone, where buffer and competition effects compensate each other, depends on the overall degradation capacity in the system. With ongoing growth, it moves closer to the NAPH source, as can be seen from intersecting biomass curves of positions B, C and D (Fig. 2). In earlier studies, the complex interplay between toxic and nutrition

effects were not seen, since NAPH bioavailability was too low to exert toxicity (Harms, 1996; Hanzel *et al.*, 2011).

Kinetic description of bacterial growth influenced by substrate toxicity and competition

Although Fig. 4 reflects an arbitrary example, the predicted relation between substrate-inhibited degradation/growth rates and bioavailability is also suitable to explain the observations made in this study. At the initial stage of the experiment (t < 8 h) cell concentrations on the individual patches do not result in bioavailability restrictions. Substrate bioavailability is similar all over the system and competition effects are rather moderate. The resulting growth rate distribution in the LCS showed moderate variability with distance to the NAPH spot source with rates accounting for 35–55% of the rates found at higher competition in HCS at all sampling locations (data not shown). We here consider this initial situation to be represented by the high bioavailability region in Fig. 4B (i.e. low values for 1/*Bn*) where the lower substrate bioavailability to individual cells in HCS has an apparent positive impact on microbial rates. At a later stage of the experiment (t > 8 h) spatial gradients and differences between HCS and LCS in the experimental growth rates are addressed to the non-monotonous dependence of the substrate inhibited growth rate on bioavailability. Figure 3 reflects average growth rates after 72 h for HCS and LCS. In the HCS continuous decrease of the growth rates is observed at increasing distances from the NAPH source. In contrast to LCS at close distance to the NAPH source however, the high competition for NAPH significantly favours bacterial growth (i.e. the bioavailability of NAPH to the PpG7 cells still appears to be on the left-hand side of the optimum as shown in Fig. 4B). At more distant locations, however, distance to the NAPH source had negative effect on NAPH bioavailability. This is reflected by decreased growth rates of strain PpG7 and, hence, proposes a bioavailability scenario as represented by the right-hand side of the optimum in Fig. 4B. Not surprisingly, such distance effect was amplified in the HCS, where competition led to limited NAPH bioavailability and subsequent lowered growth rates strain PpG7 (Fig. 3). It appears that increasing cell density led to rising competition for the NAPH, higher distance-dependent limitations of NAPH bioavailability and lowered growth rates in the system [i.e. a situation as described by the optimum (patches A and B) or the right-hand side of the optimum in Fig. 4B (patches C and D)].

Ecological relevance

Our results suggest that vapour-phase contaminant gradients may inhibit growth of pollutant-degrading bacteria

unless sufficient substrate consumption is present. This might be of a great importance for remediation of VOCs-contaminated systems like the vadose zone of terrestrial environments where degrading bacteria present at air–water or air–solid interfaces (Schäfer *et al.*, 1998) are exposed to high amounts of contaminants vapours. The data secondly underline the importance of high active biomass and concomitant effective reduction of their exposure to inhibitory (toxic) substrates in order to create environments favourable for survival, which may influence the exposure dynamics and ecology of entire microbial communities and hence actively shape environments beneficial for enhanced biodegradation. Microbial toxicity tests hence should generally take special focus on a contaminant's bioavailability and bioaccessibility in a given environment, i.e. both on its chemodynamics and on the adaptive mechanisms employed by microorganisms to avoid and/or transform toxic compounds to levels suitable for effective biotransformation.

Experimental procedures

Bacteria and culture conditions

The aerobic NAPH-degrading soil bacterium *P. putida* PpG7 (NAH7) (Dunn and Gunsalus, 1973) was grown at 25°C in 100 ml Erlenmeyer flasks containing 50 ml of liquid mineral medium (MM) on a gyratory shaker (150 r.p.m.) (Wick *et al.*, 2001) in the presence of 1.5 g l^{-1} solid NAPH (> 98%, Fluka; crystals as obtained by the provider). Inocula used for the growth experiments were harvested after 48 h of growth in the late exponential phase, centrifuged, washed twice with MM and resuspended in MM to obtain final bacterial suspension with an optical density at 600 nm (OD$_{600}$) of *c.* 0.3 corresponding to *c.* 3×10^7 cfu ml^{-1}. Cells were quantified as cfu after 3 days of incubation at room temperature on Luria Broth agar (2% w/v) using an automated spiral plating and cell counting system (Meintrup GmbH). Mineral medium agar [1.5% (w/v)] was used for growth experiments as detailed below.

Growth of P. putida (NAH7) G7 on vapour-phase NAPH

On the basis of former data (Hanzel *et al.*, 2010) growth experiments were performed at room temperature in Teflon tape-sealed, upside-down positioned Petri dishes (diameter: 9 cm) containing 20 mg of NAPH as sole carbon and energy source. NAPH was centrally placed in the lid (Fig. 1A) with solid NAPH being visible until the end of the experiment. As illustrated in Fig. 1 the Petri dishes contained a disk-shaped central MMA disk (patch A; diameter 0.5 cm) and/or three concentric, ring-shaped MMA patches (width: 0.5 cm) of increasing outer diameters (i.e. 3.4, 6.2 and 9 cm for patches B, C, D) corresponding to average distances of 1.1, 2.1, 3.3 and 4.9 cm from the NAPH point source. The total surface areas of patches A, B, C and D were 0.2 cm^2, 4.2 cm^2, 8.5 cm^2 and 12.7 cm^2 and all patches were inoculated at a density of *c.* 4.5×10^8 cfu cm^{-2} (i.e. using 5 µl of cell suspen-

sion of an OD$_{578}$ ≈ 0.3 per cm^{-2}). Two growth scenarios resulting in differential competition for the substrate were tested. In a '*high-competition experiments*' all four agar patches were placed in the same Petri dish and homogeneously inoculated whereas in the '*low-competition experiments*' each patch was placed in a separate Petri dish and inoculated (Fig. 1B). Growth of PpG7 bacteria on vapour-phase NAPH was approximated by cfu analysis after 0, 8, 20, 30, 48 and 72 h (t$_0$, t$_8$, t$_{20}$, t$_{30}$, t$_{48}$, t$_{72}$) of incubation. Therefore, the entire patch A or four equally sized and equally distributed segments (surface area: 0.75 cm^2) of each of the patches B–D were harvested. Extracted bacteria were suspended in 9 ml of PBS buffer, vortexed for 1 min, sonicated (2 × 1 min with a break of 30 s) and spread on LB plates. All experiments were performed in triplicate. Colony-forming units shown in Figs. 2–4 represent cfu averages and standard errors from three independent experiments as outlined in Fig. 1. The cfu of all platings were calculated using two different dilutions calculated according to: $cfu_{total} = [(cfu_{at\ lower\ dilution}) + (cfu_{at\ higher\ dilution}/10)]/1.1$ (Süßmuth *et al.*, 1987).

References

Ahn, I.S., Ghiorse, W.C., Lion, L.W., and Shuler, M.L. (1998) Growth kinetics of *Pseudomonas putida* G7 on naphthalene and occurrence of naphthalene toxicity during nutrient deprivation. *Biotechnol Bioeng* **59:** 587–594.

Baveye, P., and Valocchi, A. (1989) An evaluation of mathematical-models of the transport of biologically reacting solutes in saturated soils and aquifers. *Water Resour Res* **25:** 1413–1421.

Best, J.B. (1955) The interference of intracellular enzymatic properties from kinetic data obtained on living cells. I. Some kinetic considerations regarding an enzyme enclosed by a diffusion barrier. *J Cell Comp Physiol* **46:** 1–27.

Bosma, T.N.P., Middeldorp, P.J.M., Schraa, G., and Zehnder, A.J.B. (1997) Mass transfer limitation of biotransformation: quantifying bioavailability. *Environ Sci Technol* **31:** 248–252.

Button, D.K. (1991) Biochemical basis for whole-cell uptake kinetics: specific affinity, oligotrophic capacity, and the meaning of the Michaelis constant. *Appl Environ Microbiol* **57:** 2033–2038.

Dunn, N.W., and Gunsalus, I.C. (1973) Transmissible plasmid coding early enzymes of oxidation in *Pseudomonas putida*. *J Bacteriol* **114:** 974–979.

George, K.W., and Hay, A.G. (2011) Bacterial strategies for growth on aromatic compounds. *Adv Appl Microbiol* **74:** 2–25.

Hanzel, J., Harms, H., and Wick, L.Y. (2010) Bacterial chemotaxis along vapor-phase gradients of naphthalene. *Environ Sci Technol* **44:** 9304–9310.

Hanzel, J., Thullner, M., Harms, H., and Wick, L.Y. (2011) Microbial growth with vapor-phase substrate. *Environ Pollut* **159:** 858–864.

Harms, H. (1996) Bacterial growth on distant naphthalene diffusing through water, air, water-saturated, and unsaturated porous media. *Appl Environ Microbiol* **62:** 2286–2293.

Hesse, F., Harms, H., Attinger, S., and Thullner, M. (2010) Linear exchange model for the description of mass transfer limited bioavailability at the pore scale. *Environ Sci Technol* **44:** 2064–2071.

Johnsen, A.R., Wick, L.Y., and Harms, H. (2005) Principles of microbial PAH degradation. *Environ Pollut* **133:** 71–84.

Kampara, M., Thullner, M., Harms, H., and Wick, L.Y. (2009) Impact of cell density on microbially induced stable isotope fractionation. *Appl Microbiol Biotechnol* **81:** 977–985.

Lehninger, A.L., Nelson, D.L., and Cox, M.M. (2004) *Lehninger Principles of Biochemistry*, 4th edn. New York, USA: W. H. Freeman.

Monod, J. (1949) The growth of bacterial cultures. *Annu Rev Microbiol* **3:** 371–394.

Mulchandani, A., and Luong, J.H.T. (1989) Microbial inhibition-kinetics revisited. *Enzyme Microb Technol* **11:** 66–73.

Park, W., Jeon, C.O., Cadillo, H., DeRito, C., and Madsen, E.L. (2004) Survival of naphthalene-degrading *Pseudomonas putida* NCIB 9816-4 in naphthalene-amended soils: toxicity of naphthalene and its metabolites. *Appl Microbiol Biotechnol* **64:** 429–435.

Pumphrey, G.M., and Madsen, E.L. (2007) Naphthalene metabolism and growth inhibition by naphthalene in *Polaromonas naphthalenivorans* strain CJ2. *Microbiology-SGM* **153:** 3730–3738.

Schäfer, A., Harms, H., and Zehnder, A.J.B. (1998) Bacterial accumulation at the air–water interface. *Environ Sci Technol* **32:** 3704–3712.

Schwarzenbach, R.P., Gschwend, P.M., and Imboden, D.M. (2003) *Environmental Organic Chemistry*. Hoboken, NJ: John Wiley & Sons.

Simoni, S.F., Schäfer, A., Harms, H., and Zehnder, A.J.B. (2001) Factors affecting mass transfer limited biodegradation in saturated porous media. *J Contam Hydrol* **50:** 99–120.

Süßmuth, R., Eberspächer, J., Haag, R., and Springer, W. (1987) *Biochemisch-mikrobiologisches Praktikum*. Stuttgart, NY, USA: Thieme.

Thullner, M., Regnier, P., and Van Cappellen, P. (2007) Modeling microbially induced carbon degradation in redox-stratified subsurface environments: concepts and open questions. *Geomicrobiol J* **24:** 139–155.

Wick, L.Y., Colangelo, T., and Harms, H. (2001) Kinetics of mass transfer-limited bacterial growth on solid PAHs. *Environ Sci Technol* **35:** 354–361.

Supporting information

Additional Supporting Information may be found in the online version of this article:

Fig. S1. Photographs of the side (A) and birds view (B) of the experimental scenario to assess for increased inter-microbial competition ('high competition'; approximate sampling locations are symbolized by the light-coloured squares) for studying growth of surface-associated *Pseudomonas putida* (NAH7) G7 on vapour-phase NAPH. The position of NAPH addition is marked in (A), whereas letters in (B) refer to the name of the patches sampled. Please note that the Teflon-tape seals surrounding the Petri dishes were removed for better clarity of the photographs.

Fig. S2. Photographs of the birds view depicting the four scenarios to mimic lower competition scenarios ('low competition; sampling locations are symbolized by the light-coloured areas) for studying growth of surface-associated *Pseudomonas putida* (NAH7) G7 on vapour-phase NAPH prior to addition of NAPH. The position of NAPH addition is marked by the light coloured circles. Please also note that the Teflon-tape seals surrounding the Petri dishes were removed for better clarity of the photographs.

Please note: Wiley-Blackwell are not responsible for the content or functionality of any supporting materials supplied by the authors. Any queries (other than missing material) should be directed to the corresponding author for the article.